Supporting Information to:

Structural and magnetic phase transitions in the $A_nB_nO_{3n-2}$ anion-deficient perovskites $Pb_2Ba_2BiFe_5O_{13}$ and $Pb_{1.5}Ba_{2.5}Bi_2Fe_6O_{16}$

A.M. Abakumov, M. Batuk, A.A. Tsirlin, O.A. Tyablikov, D.V. Sheptyakov, D.S. Filimonov, K.V. Pokholok, V.S. Zhidal, M.G. Rozova, E.V. Antipov, J. Hadermann, G. Van Tendeloo

Table S1. Compositional dependence of the lattice parameters for the $Pb_{2-x}Ba_{2+x}Bi_2Fe_6O_{16}$ solid solutions (T = 625K).

Formula	*a*, Å	*b*, Å	*c*, Å	V, Å^3
$Pb_{1.3}Ba_{2.7}Bi_2Fe_6O_{16}$	5.80732(4)	3.98947(3)	33.1772(3)	768.65(1)
$Pb_{1.5}Ba_{2.5}Bi_2Fe_6O_{16}$	5.80362(5)	3.99049(3)	33.1391(3)	767.48(2)
$Pb_{1.7}Ba_{2.3}Bi_2Fe_6O_{16}$	5.79861(8)	3.99020(5)	33.1037(5)	765.94(3)
*$Pb_{2.0}Ba_{2.0}Bi_2Fe_6O_{16}$	5.79329(6)	3.98877(4)	33.0715(4)	764.22(2)

* - contains admixtures

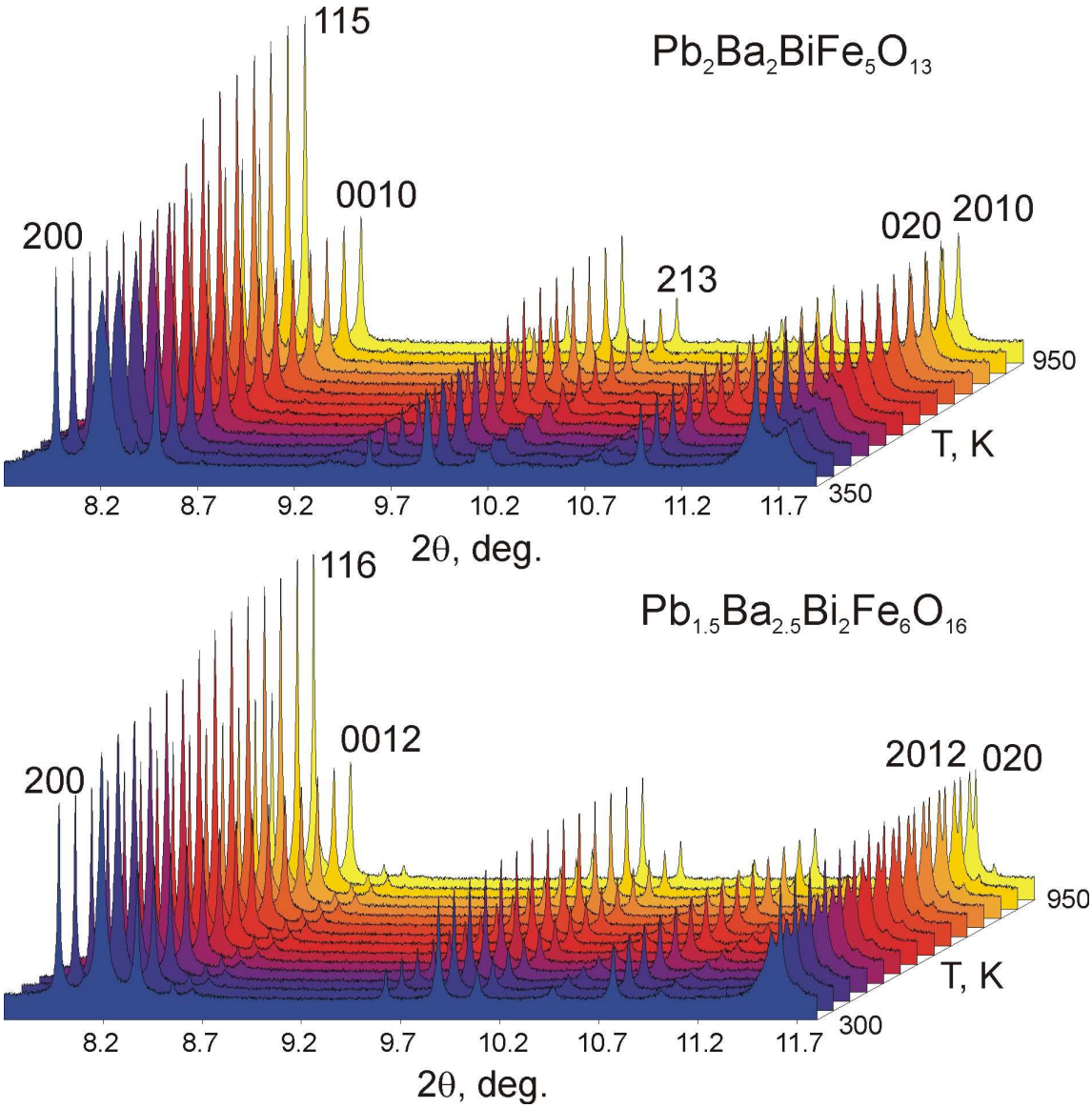

Figure S1. Temperature dependence of the synchrotron powder X-ray diffraction patterns for $Pb_2Ba_2BiFe_5O_{13}$ and $Pb_{1.5}Ba_{2.5}Bi_2Fe_6O_{16}$.

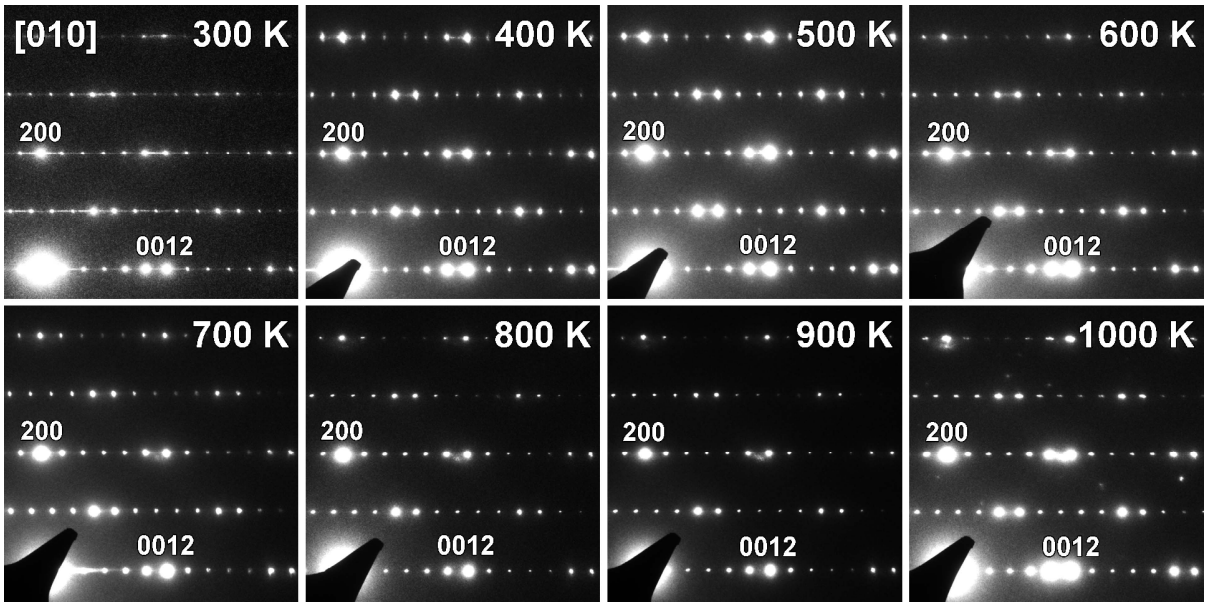

Figure S2. [010] ED patterns of $Pb_{1.5}Ba_{2.5}Bi_2Fe_6O_{16}$ at different temperatures. Note vanishing the diffuse streaks above 600K.

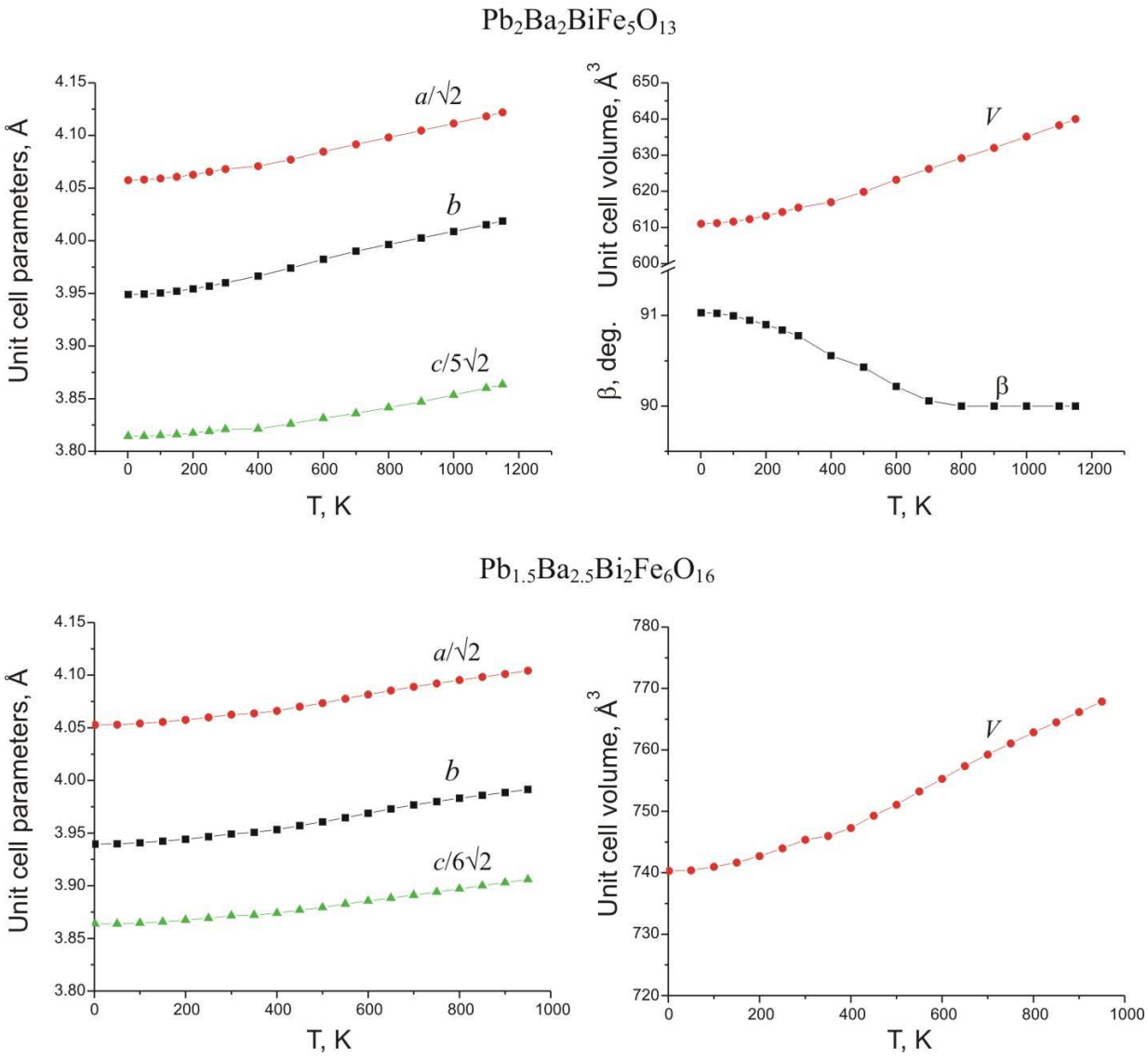

Figure S3. Temperature dependence of the lattice parameters and unit cell volume for $Pb_2Ba_2BiFe_5O_{13}$ and $Pb_{1.5}Ba_{2.5}Bi_2Fe_6O_{16}$. The small kinks at RT are due to changing the sample environment.

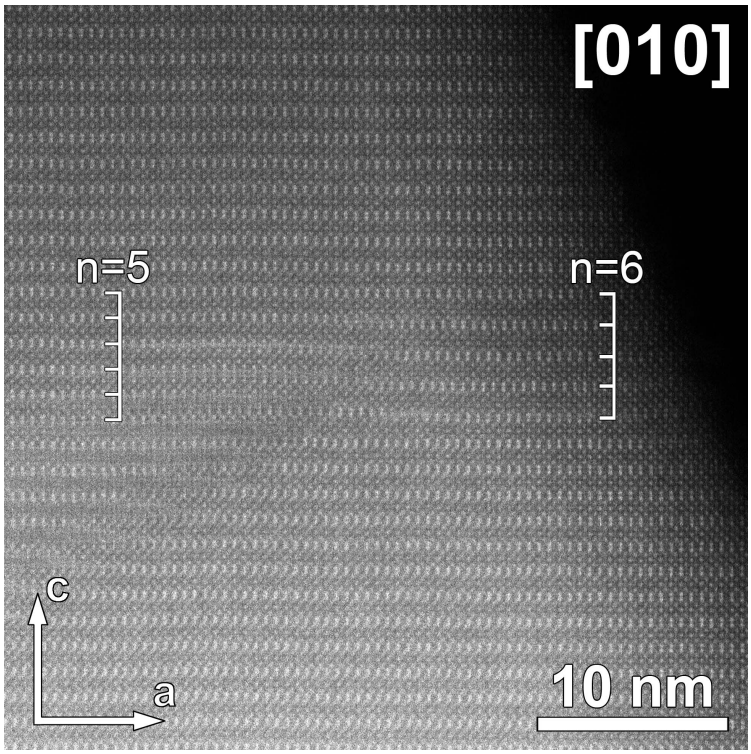

Figure S4. HAADF-STEM image of stacking faults in the $Pb_2Ba_2BiFe_5O_{13}$. The domain of the n = 6 homologue is inserted into the n = 5 matrix.

Table S2. Symmetry operators of the $P_S\bar{1}$ magnetic space group (#2.7 in Belov-Neronova-Smirnova notations).

Seitz symbol	Symmetry operator	Seitz symbol	Symmetry operator
$(1 \mid 0,0,0)$	*x, y, z, m*	$(1 \mid 0,\tfrac{1}{2},0)'$	*x*, *y*+1/2, *z*, -*m*
$(\bar{1} \mid 0,0,0)$	-*x*, -*y*, -*z*, *m*	$(\bar{1} \mid 0,\tfrac{1}{2},0)'$	-*x*, -*y*+1/2, -*z*, -*m*

Table S3. Positions of the magnetic atoms, the components of their magnetic moments and the magnetic moment values in $Pb_2Ba_2Bi_2Fe_5O_{13}$ at T = 1.5 K (magn. S.G. $P_S\bar{1}$, a = 5.7386Å, b = 7.8980Å, c = 13.6302Å, α = 98.417°, β = 91.011°, γ = 90° all m_x = 0).

Atom	x/a	y/b	z/c	m_y	m_z	M, μ_B
Fe1	0.5184	0.6033	0.4142	3.80(2)	-0.563(3)	3.85(2)
Fe2	0.5520	0.2053	0.0107	-3.80(2)	0.563(3)	3.85(2)
Fe3	1/2	0	0	-3.80(2)	0.563(3)	3.85(2)

Table S4. Symmetry operators of the B_b2/b magnetic space group (#15.90 in Belov-Neronova-Smirnova notations).

Seitz symbol	Symmetry operator	Seitz symbol	Symmetry operator
$(0,0,0)+\ (\frac{1}{2},0,\frac{1}{2})+$			
$(1\,\vert\,0,0,0)$	*x, y, z, m*	$(1\,\vert\,0,\frac{1}{2},0)'$	*x, y*+1/2, *z, -m*
$(\bar{1}\,\vert\,0,0,0)$	-*x*, -*y*, -*z*, *m*	$(\bar{1}\,\vert\,0,\frac{1}{2},0)'$	-*x*, -*y*+1/2, -*z*, -*m*
$(2_x\,\vert\,0,\frac{1}{2},0)$	*x*, -*y*+1/2, -*z*, *m*	$(2_x\,\vert\,0,0,0)'$	*x*, -*y*+1/2, -*z*, -*m*
$(m_x\,\vert\,0,\frac{1}{2},0)$	-*x*, *y*+1/2, *z*, *m*	$(m_x\,\vert\,0,0,0)'$	-*x*, *y*, *z*, -*m*

Table S5. Positions of the magnetic atoms, the components of their magnetic moments and the magnetic moment values in $Pb_{1.5}Ba_{2.5}Bi_2Fe_6O_{16}$ at T = 500 K (magn. S.G. B_b2/b, a = 5.7620Å, b = 7.9235Å, c = 33.1627Å, α = 96.868°, all m_x, m_z= 0).

Atom	*x/a*	*y/b*	*z/c*	m_y	M, μ_B
Fe1	0	0.3592	0.9646	2.63(2)	2.63(2)
Fe2	0	0.1883	0.6219	2.63(2)	2.63(2)
Fe3	0	0.2711	0.7910	2.63(2)	2.63(2)

Table S6. Symmetry operators of the P_b2/c magnetic space group (#14.80 in Belov-Neronova-Smirnova notations).

Seitz symbol	Symmetry operator	Seitz symbol	Symmetry operator
$(1\,\vert\,0,0,0)$	*x, y, z, m*	$(1\,\vert\,0,\tfrac{1}{2},0)'$	*x, y*+1/2, *z, -m*
$(\bar{1}\,\vert\,0,0,0)$	-*x*, -*y*, -*z*, *m*	$(\bar{1}\,\vert\,0,\tfrac{1}{2},0)'$	-*x*, -*y*+1/2, -*z*, -*m*
$(2_x\,\vert\,\tfrac{1}{2},0,\tfrac{1}{2})$	*x*+1/2, -*y*, -*z*+1/2, *m*	$(2_x\,\vert\,\tfrac{1}{2},\tfrac{1}{2},\tfrac{1}{2})'$	*x*+1/2, -*y*+1/2, -*z*+1/2, -*m*
$(m_x\,\vert\,\tfrac{1}{2},0,\tfrac{1}{2})$	-*x*+1/2, *y*, *z*+1/2, *m*	$(m_x\,\vert\,\tfrac{1}{2},\tfrac{1}{2},\tfrac{1}{2})'$	-*x*+1/2, *y*+1/2, *z*+1/2, -*m*

Table S7. Positions of the magnetic atoms, the components of their magnetic moments and the magnetic moment values in $Pb_{1.5}Ba_{2.5}Bi_2Fe_6O_{16}$ at T = 1.5 K (magn. S.G. P_b2/c, a = 5.7620Å, b = 7.9235Å, c = 33.1627Å, α = 96.868°, all m_x, m_z= 0).

Atom	*x/a*	*y/b*	*z/c*	m_y	M, μ_B
Fe1	0.5091	0.1061	0.4651	3.90(2)	3.90(2)
Fe2	0.5192	0.9382	0.1224	3.90(2)	3.90(2)
Fe3	0.5198	0.0179	0.2922	3.90(2)	3.90(2)

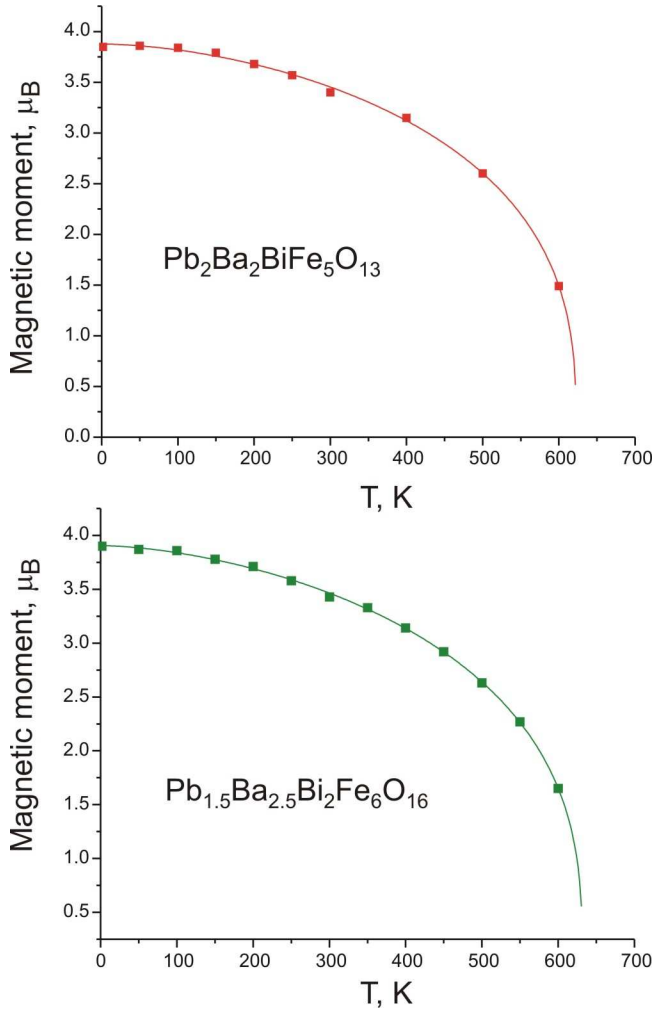

Figure S5. Temperature dependence of the magnetic moments for $Pb_2Ba_2BiFe_5O_{13}$ and $Pb_{1.5}Ba_{2.5}Bi_2Fe_6O_{16}$. The lines are the fit with the $M = M_0(1 - (T/T_N)^{\alpha})^{\beta}$ function.

Table S8. The ^{57}Fe Mössbauer hyperfine parameters for $Pb_2Ba_2BiFe_5O_{13}$: magnetic hyperfine field H, isomer shift relative to α-Fe δ, electric quadrupole splitting ΔE_Q, apparent quadrupole shift 2ε, full width at half maximum Γ of individual components, relative absorption areas A.

T (K)	*Comp.*	H (T)	δ (mm s^{-1})	ΔE_Q (mm s^{-1})	2ε, (mm s^{-1})	Γ (mm s^{-1})	A (%)
		±0.5	±0.03	±0.03	± 0.03	±0.01	±2
558	A1	-	0.17	0.33	-	0.31	60
	B1	-	0.15	0.57	-	0.29	40
78	A2	55.6	0.47	-	-0.25	0.33	14
	A3	54.5	0.45	-	-0.22	0.34	24
	A4	53.5	0.54	-	-0.40	0.36	21
	B2	51.1	0.42	-	0.20	0.32	23
	B3	50.2	0.41	-	0.25	0.27	13
	B4	48.8	0.40	-	0.20	0.36	5

Table S9. Atomic coordinates and parameters of the crenel functions for the ordered alternation of the ABO_2 and O_2 layers in the $A_nB_nO_{3n-2}$ homologues (superspace group *Xmmm*(00γ)000 (X = [1/2, 0, 1/2, 0]; [0, 1/2, 1/2, 1/2]; [1/2, 1/2, 0, 1/2], $a = a_p\sqrt{2}$, $b = a_p$, $c = a_p\sqrt{2}$, $\mathbf{q} = \gamma\mathbf{c}^*$ ($\gamma = 1/n$)). The $A_nB_nO_{3n-2}$ structures can be derived as commensurate approximants with $c' = c/\gamma = nc$ with *Ammm* (*n* - odd) and *Imma* (*n* - even) space symmetries for special values of the initial modulation phase $t = \frac{p}{2n}$ and $t = \frac{2p+1}{4n}$ (*p* - integer), respectively.

Atom	*x/a*	*y/b*	*z/c*	x_4^0	Δ
A1	0	0	0	1/2	1/2 - γ
A2	0	0	0	(3 - γ)/4	γ/2
B1	0	0	0	0	1/2 - γ
B2	0	0	0	(1 - γ)/4	γ/2
O1	0	1/2	0	0	1/2 - γ
O2	1/4	0	1/4	0	(1 - γ)/2
O3	0	1/2	0	(1 - γ)/4	γ/2

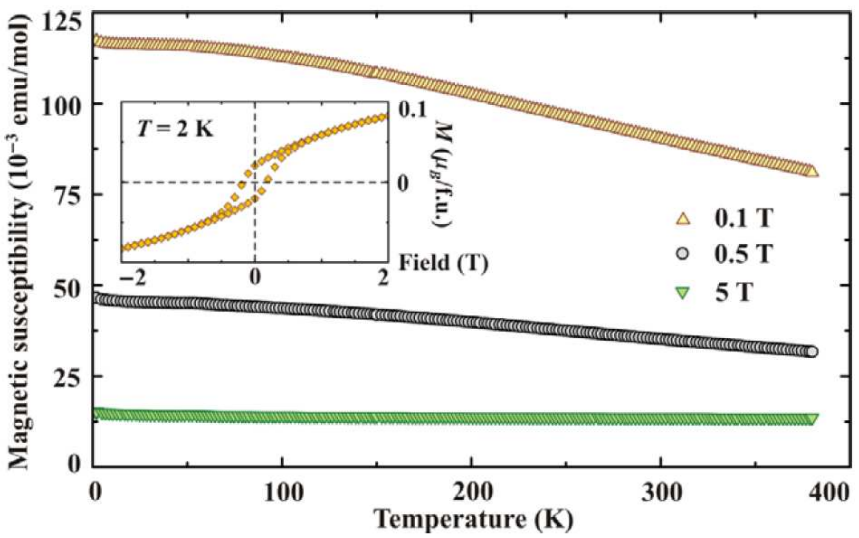

Figure S6. Magnetic susceptibility of the pristine $Pb_{1.5}Ba_{2.5}Bi_2Fe_6O_{16}$ sample. The inset shows the magnetization curve measured at 2 K. Note the small hysteresis with the net moment of about 0.04 μ_B/f.u.

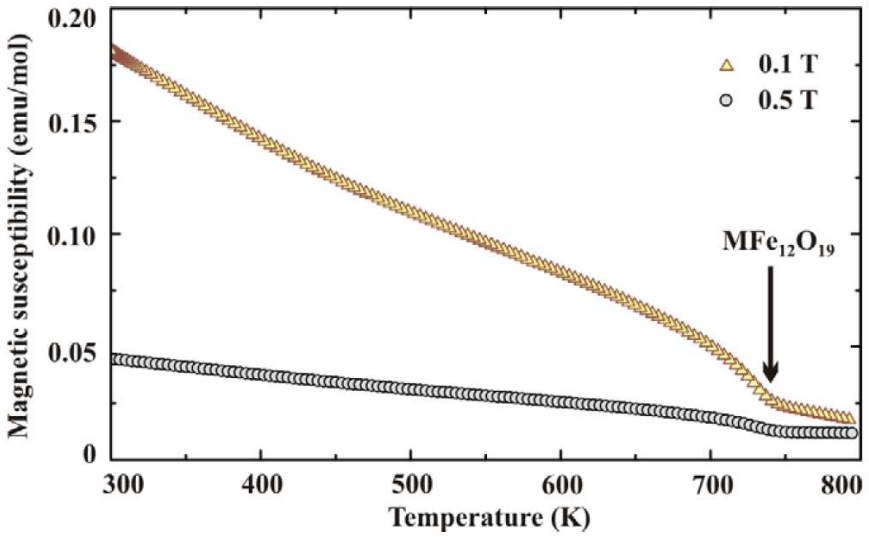

Figure S7. High-temperature magnetic susceptibility of $Pb_{1.5}Ba_{2.5}Bi_2Fe_6O_{16}$. Absolute values of the magnetic susceptibility are different from those in Fig. S4, because cycling up to 800 K leads to a marginal decomposition toward Fe_3O_4 that increases the magnetization (see text for details). The presence of ferrimagnetic Fe_3O_4 is also responsible for the small difference between the 0.1 T and 0.5 T data above 730 K, where other ferromagnetic impurities, such as $MFe_{12}O_{19}$ hexaferrites, become paramagnetic.